JOURNAL OF CHEMICAL & ENGINEERING DATA

ARTICLE

pubs.acs.org/jced

Adsorption Kinetics and Isotherms of Ag(I) and Hg(II) onto Silica Gel with Functional Groups of Hydroxyl- or Amino-Terminated Polyamines

Rongjun Qu,*[,†] Minghua Wang,[†] Renfeng Song,[‡] Changmei Sun,[†] Ying Zhang,[†] Xiaoying Sun,[†] Chunnuan Ji,[†] Chunhua Wang,[†] and Ping Yin[†]

[†]School of Chemistry and Materials Science, Ludong University, Shandong 264025, China

[‡]An'gang Group Mining Engineering Corporation, Liaoning 114002, China

ABSTRACT: Five kinds of silica-gel adsorbents with functional groups of hydroxyl- or amino-terminated polyamines (SiO_2-EA, SiO_2-DEA, SiO_2-EDA, SiO_2-DETA, and SiO_2-TETA), whose structures of functional groups were characterized according to the results of elemental analysis, were chosen to investigate the adsorption kinetics and isotherms toward Ag(I) and Hg(II). The results of the kinetics adsorption showed that all of the adsorption processes followed a pseudo-second-order model, suggesting that the five adsorbents can be applied in Ag(I) and Hg(II) removal from lower concentration solutions. Film diffusion might dominate in the adsorption process of Ag(I) and Hg(II) onto the five adsorbents. The linear and nonlinear Langmuir, Freundlich, and Redlich−Peterson models were employed to fit the isothermal adsorptions. The results revealed that all the above-mentioned isotherm models can be used to predict the experimental data. The relationship between the structure of functional groups and the adsorption mechanism is also discussed.

1. INTRODUCTION

With increasing industrialization, a large number of toxic metals have entered the environment with the discharge of industrial wastewater. Treatment of contaminated water drainage is a critical environmental issue due to the potential for heavy metals to enter drinking water resources. Furthermore, even low levels of heavy metals can be concentrated to dangerous levels through the natural process of bioaccumulation.

Silver in wastewater can be accumulated in organisms (including humans) through the food chain and cause numerous diseases and disorders. Moreover, as a raw material, silver was widely used in industries due to its excellent malleability, ductility, electrical and thermal conductivity, photosensitivity, and antimicrobial properties. Therefore, removal and separation of silver from wastewater discharged from industries is important because of the toxicity of silver to living organisms.[1]

Mercury-containing wastewater is generated from metallurgical, metal finishing, and chemical manufacturing industries. Mercury can exist in aqueous solutions in various forms, but the main species is Hg(II),[2] which can easily bind to organic and inorganic matter in aqueous solution and pose a significant threat to aquatic life and render natural water unsuitable for public use.[3,4] So, treatment of the resulting Hg(II)-laden water drainage is also a critical environmental issue.

Various methods such as adsorption, solvent extraction, and polymeric membranes have been proposed to remove heavy metals from the environment.[5−8] Each of these methods has some merits and limitations in practice. Chelating adsorption has proved to be one of the most promising methods among the above-mentioned methods. Chelating adsorbents are generally efficient in the removal and recovery of heavy metal ions because of their physical and chemical stabilities.[9] As a low-cost inorganic polymer material, silica gel serves as a potentially useful candidate for producing adsorbents due to its particular structure and unique characteristics of no swelling, good mechanical stability, and rapid kinetics.[10] In addition, the unique large surface area, well-defined pore size and pore shape, and well-modified surface properties have generated considerable interest in the fabrication of many novel silica-gel-based adsorbents.[11−14]

Among the silica-gel-based chelating adsorbents, the nitrogen-type chelating resins using nitrogen atoms as ligating atoms have excellent adsorption properties for heavy-metal ions.[15−17] Especially the chelating adsorbents containing multi-amino-typed functional groups are capable of coordinating to heavy metal ions to form multidentate chelates owing to a great deal of amino groups existing in the molecules, together with their fine hydrophilicity.[18−23]

Recently, we synthesized five novel adsorbents, SiO_2-EA, SiO_2-DEA, SiO_2-EDA, SiO_2-DETA, and SiO_2-TETA, by supporting polyamines such as ethanolamine (EA), diethanolamine (DEA), ethylenediamine (EDA), diethylenetriamine (DETA), and triethylenetetramine (TETA), respectively, on the surface of silica gel through amido bonds.[24] Moreover, we investigated the adsorption of these adsorbents for Au(III) in aqueous solution.

In the present paper, the kinetics and isotherms of the five adsorbents for Ag(I) and Hg(II) adsorption were investigated in order to understand the relationship between the structure and adsorption efficiency and to expand the application of these adsorbents in removal of metals from wastewater. Furthermore, the effects of terminal groups on the adsorption mechanisms were also discussed by comparing the kinetics and isotherm parameters.

Received: September 29, 2010
Accepted: February 25, 2011
Published: March 15, 2011

dx.doi.org/10.1021/je1009784 | *J. Chem. Eng. Data* 2011, 56, 1982–1990

2. EXPERIMENTAL SECTION

2.1. Materials and Methods. Adsorbents SiO_2-EA, SiO_2-DEA, SiO_2-EDA, SiO_2-DETA, and SiO_2-TETA were prepared according to the method described in our previous work.[24] The synthetic routes are illustrated in Scheme 1.

The elemental analysis data are listed in Table 1. The BET surface area was found to be (192.65, 156.50, 147.37, 127.60, and 114.91) m^2/g, and the BJH desorption average pore diameter was (6.18, 6.20, 5.69, 5.42, and 5.16) nm for SiO_2-EA, SiO_2-DEA, SiO_2-EDA, SiO_2-DETA, and SiO_2-TETA, respectively. A solution of 0.002 mmol L^{-1} of Ag(I) was prepared using analytical grade $AgNO_3$. A 0.002 mmol L^{-1} solution of Hg(II) was prepared by dissolving a desired amount of analytical grade $Hg(NO_3)_2 \cdot H_2O$ in 0.6 % HNO_3. The initial pH of the solution was adjusted to 4.0 according to our previous work.[23] All other solutions were diluted from these stock solutions. The concentration before and after adsorption of the metal ions was determined using a 932B-model atomic adsorption spectrophotometer (AAS, GBC, Australia), equipped with an air−acetylene flame.

2.2. Adsorption Kinetics. A batchwise process was employed in the adsorption of Ag(I) and Hg(II) on the five silica-gel adsorbents from aqueous solution. The adsorption procedure can be described as follows: a definite amount of the silica-gel adsorbents was added into several 100 mL Erlenmeyer flasks, each containing 20 mL of a metal ion solution. The flasks were then shaken at 25 °C for a predetermined time. After the prescribed contact time, the solid adsorbents were filtered off, and the metal ion concentrations in the solutions were determined via AAS.

Scheme 1. Synthetic Routes of Hydroxyl- and Amino-Terminated Polyamine Grafted Silica Gel

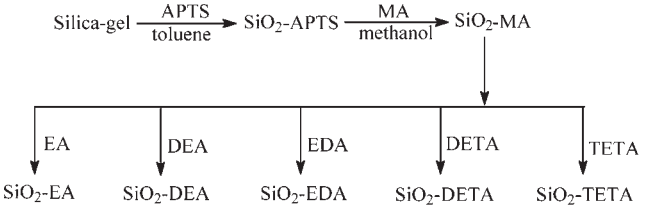

APTS=Aminopropyltrimethoxysilane; MA=Metyl acrylate; EA=Ethanolamine DEA=Diethanolamine; EDA=Ethylenediamine; DETA=Diethylenetriamine; TETE=Triethlyenetetramine

2.3. Adsorption Isotherms. Complete adsorption equilibrium was obtained by soaking 40 mg of the dry silica-gel adsorbent in a series of Erlenmeyer flasks containing 20 mL of a metal ion solution for 20 h at 25 °C. The solid adsorbents were filtered off and the metal ion concentrations in the solutions determined via AAS. The amount of metal ions adsorbed at equilibrium q, which represents the metal ion uptake, was calculated according to eq 1:

$$q = \frac{(C_0 - C)V}{W} \quad (1)$$

where q is the adsorption amount (mmol g^{-1}), C_0 and C are the initial and final concentrations of metal ions in aqueous solution, respectively (mmol L^{-1}), V is the volume (L), and W is the weight of the adsorbent (g).

2.4. Primary Desorption. Primary desorption experiments were carried out as follows: after adsorption, the metal ion loaded adsorbents were separated and slightly washed with distilled water to remove unadsorbed metal ions on the surface of the adsorbents. Then, they were stirred with 20 mL of 5 % thiourea/0.5 mol L^{-1} HNO_3 for 20 h. Concentrations of metal ions in aqueous solutions were analyzed as before. The desorption ratio of the metal ion was then calculated as the ratio of the amount of desorbed metal ion to the amount of initially adsorbed metal ion.

3. RESULTS AND DISCUSSION

3.1. Structure Analysis. The species and content of functional groups of an adsorbent is an important factor affecting its adsorption properties and adsorption mechanism. In previous work, the physical properties of the five adsorbents were characterized.[24] In this paper, the structures and content of the functional groups of the five adsorbents were analyzed according to elemental analysis data. Theoretically, in the coupling reaction of γ-aminopropyltrimethoxysilane (APTS) with silica gel, the three methoxy groups of APTS can react with one, two, or three silanol groups on the surface of the silica gel to obtain SiO_2-APTS

Scheme 2. Possible Structures of SiO_2-APTS

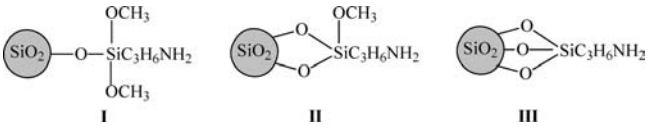

Table 1. Elemental Analysis Data and Functionalization Degrees of Silica Gels

	C	N		functional groups content	theoretical functional groups content
samples	(%)	(%)	C/N[a]	(mmol g^{-1})[b]	(mmol g^{-1})[c]
SiO_2-APTS	10.21	2.79	4.27	1.99	
SiO_2-MA	13.71	2.38	6.72	2.03	
SiO_2-EA	13.50	3.42	4.61	0.80	1.92
SiO_2-DEA	12.08	3.09	4.56	0.60	1.77
SiO_2-EDA	13.33	4.75	3.28	0.89	1.92
SiO_2-DETA	15.26	5.50	3.24	0.82	1.77
SiO_2-TETA	16.36	5.81	3.28	0.70	1.65

[a] C/N = mmol·g^{-1} C/mmol·g^{-1} N. [b] Functional group means NH_2, CO_2CH_3, EA, DEA, EDA, DETA, and TETA for SiO_2-APTS, SiO_2-MA, SiO_2-EA, SiO_2-DEA, SiO_2-EDA, SiO_2-DETA, and SiO_2-TETA, respectively. [c] Theoretical functional group content = theoretical values of millimoles of ligand per gram of functionalized silica gel, which are calculated according to the $-CO_2CH_3$ content in SiO_2-MA.

dx.doi.org/10.1021/je1009784 |J. Chem. Eng. Data 2011, 56, 1982–1990

Table 2. *Bt* Versus Time Linear Equations and Coefficients R^2

metal ions	adsorbents	linear equation	coefficient of determination, R^2
Ag(I)	SiO_2-EA	$Bt = 0.51448t - 0.01321$	0.9910
	SiO_2-DEA	$Bt = 0.37043t + 0.04262$	0.9990
	SiO_2-EDA	$Bt = 0.38162t + 0.11322$	0.9888
	SiO_2-DETA	$Bt = 0.30978t + 0.02031$	0.9839
	SiO_2-TETA	$Bt = 0.28136t - 0.04405$	0.9845
Hg(II)	SiO_2-EDA	$Bt = 0.67553t + 0.15107$	0.9957
	SiO_2-DETA	$Bt = 0.62470t - 0.01250$	0.9232
	SiO_2-TETA	$Bt = 0.73094t + 0.11886$	0.9093

Scheme 3. Possible Structures of SiO_2-MA

Scheme 4. Possible Structures of SiO_2-EDA, SiO_2-DETA, and SiO_2-TETA

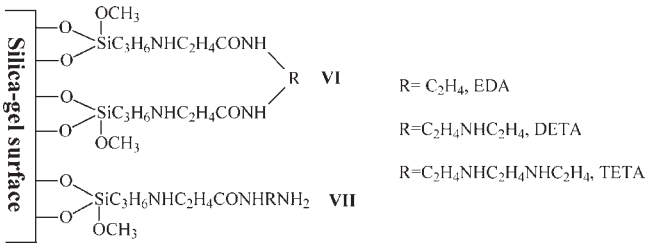

with three kinds of structures, which is illustrated in Scheme 2. According to the 4.27:1 molar ratio of C/N shown in Table 2, it can be presumed that **II** was the dominant structure of SiO_2-APTS. Compared with the two possible structures of SiO_2-MA in Scheme 3, it was easy to find that the molar ratio 6.72:1 of C/N of SiO_2-MA (methyl acrylate) was nearer to the 8:1 of **IV** than to the 12:1 of **V**, implying that **IV** was the dominant structure in SiO_2-MA. The molar ratio of $-CO_2CH_3$ in SiO_2-MA (2.03) to $-NH_2$ in SiO_2-APTS (1.99) being approximately 1.02 could corroborate that **IV** was the dominant structure in SiO_2-MA.

After the amidation reaction of SiO_2-MA with the polyamines, the structures of modified silica gel became complicated due to multiple reactive sites in the molecular structure of the polyamines. According to the same method, the content of functional groups of SiO_2-EDA, SiO_2-DETA, and SiO_2-TETA could be calculated to be (0.89, 0.82, and 0.70) mmol·g^{-1}, respectively, which are much lower than their corresponding theoretical values of (1.92, 1.77, and 1.65) mmol·g^{-1}. In other words, their measured contents of functional groups were only 1/2.23, 1/1.98, and 1/2.37, respectively, of their theoretical ones. Considering that the ester groups were confirmed by FTIR to be converted completely,[24] it was reasonable to conclude that a lot of cross-linking exists in the molecular structures of SiO_2-EDA, SiO_2-DETA, and SiO_2-TETA due to the reaction of one molecule

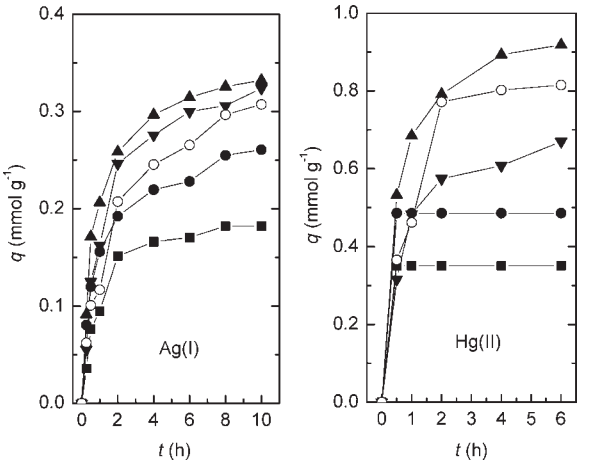

Figure 1. Adsorption kinetics of Ag(I) and Hg(II) onto adsorbents ■, SiO_2-EA; ●, SiO_2-DEA(); ▲, SiO_2-EDA(); ▼, SiO_2-DETA; and ○, SiO_2-TETA. Adsorption conditions: weights of adsorbents were 80 and 100 mg for Ag(I) and Hg(II), respectively.

of polyamine with more than one ester group. The cross-linking and chain functional groups in SiO_2-EDA, SiO_2-DETA, and SiO_2-TETA are illustrated as **VI** and **VII** in Scheme 4.

3.2. Adsorption Kinetics. Adsorption kinetics are one important characteristic that defines the efficiency of adsorption. In the present study, the kinetics of Ag(I) and Hg(II) removal were determined to understand the adsorption behaviors of adsorbents with functional groups of hydroxyl-terminated (SiO_2-EA and SiO_2-DEA) and amino-terminated (SiO_2-EDA, SiO_2-DETA, and SiO_2-TETA) polyamines, respectively. The effect of contact time at optimum pH and room temperatures (25 °C) is shown in Figure 1. As the kinetic curves in Figure 1 showed, SiO_2-EA, SiO_2-DEA, SiO_2-EDA, SiO_2-DETA, and SiO_2-TETA exhibited different adsorption characteristics for Ag(I) and Hg(II). For Ag(I), the adsorption was rapid for the first 2 h and then slowed considerably. It required about (8 to 9) h to reach adsorption equilibrium. For Hg(II), the five adsorbents exhibited faster adsorption than for Ag(I). They achieved equilibrium within 6 h. It is noteworthy that Hg(II) adsorption onto SiO_2-EA and SiO_2-DEA needed only 1 h to reach the equilibrium. Hence, in the present study, we used a 20 h contact time for further experiments in order to ensure complete adsorption.

Following Boyd et al.[25] and Reichenberg,[26] the adsorption procedure of adsorbents for metal ions was considered to take place through two mechanisms of film diffusion and particle diffusion. Film diffusion was rate controlling when the absorbent was exposed to a low metal ion concentration, and particle diffusion might be rate controlling at a high metal ion concentration. The kinetic data in Figure 1 were analyzed using the procedure given by Reichenberg[26] and Helfferich.[27] The following equations were used:

$$F = 1 - \frac{6}{\pi^2}\sum_{n=1}^{\infty}\frac{1}{n^2}\left[\frac{-D_i t\pi^2 n^2}{r_0^2}\right] \quad (2)$$

or

$$F = 1 - \frac{6}{\pi^2}\sum_{n=1}^{\infty}\frac{1}{n^2}\exp[-n^2 Bt] \quad (3)$$

where F is the fractional attainment of equilibrium at time t and is

dx.doi.org/10.1021/je1009784 |J. Chem. Eng. Data 2011, 56, 1982–1990

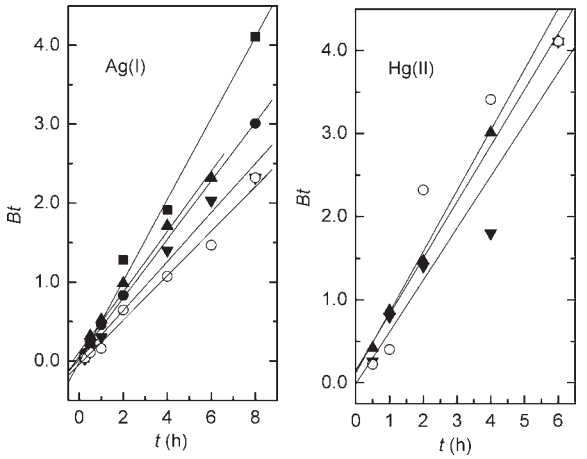

Figure 2. *Bt* vs time plots of Ag(I) and Hg(II) onto adsorbents. ■, SiO_2-EA; ●, SiO_2-DEA; ▲, SiO_2-EDA; ▼, SiO_2-DETA; and ○, SiO_2-TETA.

obtained by the expression:

$$F = \frac{q_t}{q_e} \tag{4}$$

where q_t is the amount of metal ions taken up at time t and q_e is the amount of metal ion adsorbed at equilibrium and

$$B = \frac{\pi^2 D_i}{r_0^2} = \text{time constant} \tag{5}$$

where D_i is the effective diffusion coefficient of an ion in the adsorbent phase; r_0 is the radius of the adsorbent particle, assumed to be spherical; and n is an integer that defines the infinite series solution.

Values of *Bt* were obtained from corresponding values of *F*. *Bt* values for each *F* are given by Reichenberg,[26] and the results are plotted in Figure 2.

The linearity of this plot is employed to distinguish between external-transport- (film diffusion) and intraparticle-transport-controlled rates of adsorption.[28] A straight line passing through the origin is indicative of adsorption processes governed by particle-diffusion mechanisms; otherwise, they might be governed by film diffusion.[29]

As shown in Figure 2, the lines of the relationship between *Bt* and *t* were linear for Ag(I) adsorption on all of the adsorbents and approximately linear for Hg(II) adsorption ($R^2 > 0.90$). In all cases studied, all lines of the relationships did not pass through the origin, suggesting that film diffusion, rather than the particle diffusion, is the rate-limiting adsorption process of SiO_2-EA, SiO_2-DEA, SiO_2-EDA, SiO_2-DETA, and SiO_2-TETA for Ag(I) and Hg(II). That is, the five adsorbents can be used in solution adsorption with low metal ion concentrations. The linear equations and coefficients of determination R^2 are given in Table 2.

Kinetic models can be helpful in understanding the mechanism of metal adsorption and evaluate the performance of the adsorbents for metal removal. Several kinetic models have been developed to describe the kinetics of heavy metal removal. Among them, the pseudo-first-order kinetic model of Barkat et al.[30] and pseudo-second-order kinetic model of Ho et al.[31] are the most typical ones. In this study, the pseudo-first-order and pseudo-second-order models were used to test the experimental data and thus elucidate the adsorption kinetic process. The pseudo-first-order model is expressed as

$$\ln \frac{(q_e - q_t)}{q_e} = -k_1 t \tag{6}$$

where k_1 is the pseudo-first-order rate constant (h^{-1}) of adsorption and q_e and q_t (mmol g^{-1}) are the amounts of metal ion adsorbed at equilibrium and time t (h), respectively. The value of $\ln(q_e - q_t)$ was calculated from the experimental results and plotted against t (h). The experimental and calculated q_e values, pseudo-first-order rate constants, and regression coefficient (R_1^2) values are presented in Table 3.

The pseudo-second-order model can be expressed as

$$\frac{t}{q_t} = \frac{1}{k_2 q_e^2} + \frac{t}{q_e} \tag{7}$$

where k_2 is the pseudo-second-order rate constant of adsorption (g $mmol^{-1}$ h^{-1}). The slope and intercept of the linear plot t/q_t vs t yielded the values of q_e and k_2. The regression coefficient (R^2) and several parameters obtained from the pseudo-second-order kinetic model are also shown in Table 3.

As can be seen from Figure 3 and Table 3, the pseudo-second-order model fits the data very well and provided better coefficients of determination than the pseudo-first-order model for the adsorption of Ag(I) and Hg(II) onto SiO_2-EA, SiO_2-DEA, SiO_2-EDA, SiO_2-DETA, and SiO_2-TETA, suggesting that the pseudo-second-order model was more suitable for describing the adsorption kinetics of the two metal ions onto the five adsorbents. Moreover, the calculated q_e values from the pseudo-second-order model were in good agreement with the experimental values q_e(exp).

The pseudo-second-order model assumes that two reactions are occurring. The first one is fast and reaches equilibrium quickly, and the second is a slower reaction that can continue for long time periods. The reactions can occur either in series or in parallel.[32] The fact that all of the adsorption processes fit the pseudo-second-order model indicates that the five adsorbents prepared in this paper can be applied in lower metal concentration solutions. This is in accordance with the results obtained by the aforementioned Boyd and Reichenberg equations.

From Table 3, some conclusions can be drawn from the k_2 values: (1) For the hydroxyl-terminated adsorbents SiO_2-EA and SiO_2-DEA, their rate constants for Ag(I) were obviously higher than those of their counterpart amino-terminated adsorbents (the adsorption rates of Hg(II) onto SiO_2-EA and SiO_2-DEA were too fast to be shown in Table 3). A possible reason for this is that the metal-binding capability of adsorbents terminated by amino groups is stronger than those terminated by hydroxyl groups. So the initial binding of the metal ion on the surface of amino-terminated adsorbents effectively blocks access to deeper sites, which affects the adsorption rate to a certain extent and prolongs the time to reach adsorption equilibrium. (2) For the amino-terminated adsorbents SiO_2-EDA, SiO_2-DETA, and SiO_2-TETA, the order of adsorption rates for Ag(I) ions is SiO_2-EDA > SiO_2-DETA > SiO_2-TETA. This order is inversely correlated with the nitrogen content of the adsorbents (section 2.1), meaning that the adsorption rate decreases with an increase in the length of the polyamine. A similar conclusion can be gained from the adsorption rates of Hg(II) onto SiO_2-EDA and SiO_2-DETA being much higher than onto SiO_2-TETA. This fact may be interpreted as the adsorbent with a longer chain polyamine having more cross-linking structures, which hinder the functional

Table 3. Kinetic Parameters for the Adsorption of Ag(I) and Hg(II) onto SiO_2-EA, SiO_2-DEA, SiO_2-EDA, SiO_2-DETA, and SiO_2-TETA Adsorbents

			pseudo-first-order kinetics			pseudo-second-order kinetics			
		q_e(exp)	k_1	q_e(cal)	h_1	k_2	q_e(cal)	h_2	
metal ions	adsorbents	(mmol g^{-1})	(h^{-1})	(mmol g^{-1})	(mmol g^{-1} h^{-1})	(g $mmol^{-1}$ h^{-1})	(mmol g^{-1})	(mmol g^{-1} h^{-1})	R_2^2
Ag(I)	SiO_2-EA	0.18	0.59	0.14	0.11	5.33	0.21	0.18	0.9976
	SiO_2-DEA	0.26	0.41	0.17	0.10	4.61	0.28	0.31	0.9959
	SiO_2-EDA	0.33	0.41	0.18	0.14	4.12	0.35	0.45	0.9995
	SiO_2-DETA	0.32	0.40	0.23	0.13	2.52	0.36	0.26	0.9978
	SiO_2-TETA	0.31	0.39	0.26	0.12	1.96	0.35	0.18	0.9932
Hg(II)	SiO_2-EDA	0.92	0.76	0.54	0.698	2.26	0.99	1.90	0.9998
	SiO_2-DETA	0.67	0.46	0.33	0.301	2.34	0.73	1.05	0.9972
	SiO_2-TETA	0.82	1.06	0.71	0.863	1.43	0.93	0.94	0.9900

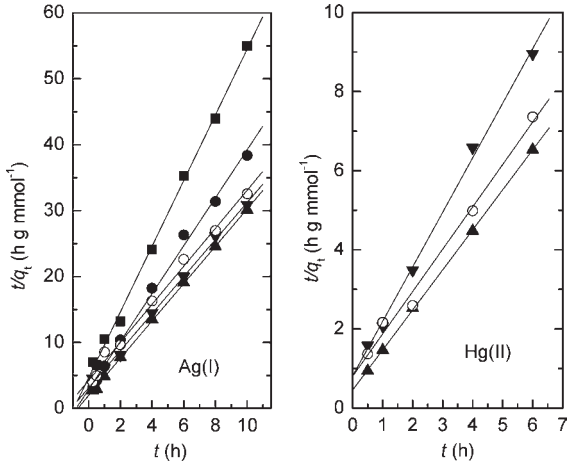

Figure 3. Pseudo-second-order kinetic plots for the adsorption of Ag(I) and Hg(II) onto adsorbents ■, SiO_2-EA; ●, SiO_2-DEA; ▲, SiO_2-EDA; ▼, SiO_2-DETA; and ○, SiO_2-TETA.

atoms coordinating with metal ions. On the other hand, the decrease in BET surface area and BJH desorption average pore diameter with an increase in the chain length of polyamine (section 2.1) makes it difficult for metal ions to diffuse into the inside of the adsorbents, which may be another reason leading to the decrease in the adsorption rate.

The initial adsorption rate, h, has been widely used for the evaluation of adsorption rates. On the basis of the pseudo-first-order and pseudo-second-order models, the initial adsorption rates (h_1, mmol g^{-1} h^{-1} and h_2, mmol g^{-1} h^{-1}) of the five adsorbents for the two metal ions are given in Table 3 according to eqs 8 and 9:[33]

$$h_1 = k_1 q_e \quad (8)$$

$$h_2 = k_2 q_e^2 \quad (9)$$

Because the adsorption obeys pseudo-second-order kinetics, the initial adsorption behavior of the metal ions onto the five adsorbents can be investigated via comparison of the h_2 values. As shown in Table 3, the initial adsorption rate, h_2, of the three amino-terminated adsorbents exhibited similar regularities to those of their adsorption rates; that is, the order of h_2 is SiO_2-EDA > SiO_2-DETA > SiO_2-TETA. This fact indicated that the cross-linking degree of the functional groups on the surface of the adsorbents affected not only the diffusion of metal ions into the inside of adsorbents (adsorption rate) but also the initial adsorption rate. From Table 3, it is easy to find the role the terminal groups played in the adsorption process via comparison of the h_2 values of Ag(I) adsorption onto SiO_2-EA and SiO_2-EDA, which have the most similar structure of functional groups, except the terminal groups. Obviously, for Ag(I) adsorption, the h_2 value of SiO_2-EDA was higher than that of SiO_2-EA, implying that the amino group has a stronger capability of capturing Ag(I) ions than hydroxyl. For the adsorption of Ag(I) onto SiO_2-EA and SiO_2-EDA, it should be noted that the rate constant of SiO_2-EA was higher than that of SiO_2-EDA, but the initial adsorption rate of the former was lower. A possible explanation for this is that abundant amines distributed on the surface of SiO_2-EDA captured Ag(I) quickly and formed complexes in the initial adsorption, which prevented other Ag(I) from diffusing into the inside of the pores of the adsorbent, so the rate constant was lower.

A conclusion can be drawn from the analysis above that the terminal group types and cross-linking structure of the functional groups have a significant effect on the adsorption rate and initial rate of metal ions onto the adsorbents.

3.3. Adsorption Isotherms. Adsorption data for a wide range of adsorbate concentrations are most conveniently described by adsorption isotherms. Linear regression is frequently used to determine the best fitting isotherm. However, previously, researchers have shown that, depending on the way isotherm equations are linearized, the error distribution changes for either the worse or the better.[34] Therefore, it is inappropriate to use a linearization method for estimating equilibrium isotherm parameters. In the present study, a comparison of the linear method and nonlinear method of three isotherms, Langmuir, Freundlich and Redlich−Peterson, were employed to determine the adsorption isotherm parameters of Ag(I) and Hg(II) onto SiO_2-EA, SiO_2-DEA, SiO_2-EDA, SiO_2-DETA, and SiO_2-TETA. The adsorption isotherms for Ag(I) and Hg(II) are presented in Figure 4. For the nonlinear method, a trial and error procedure, which is applicable to computer operation, was developed to determine the isotherm parameters by maximizing the respective coefficients of determination between the experimental data and isotherms using the Origin software.

The Langmuir equation relates the coverage of molecules on a solid surface to the concentration of a medium above the solid surface at a fixed temperature. It represents one theoretical

treatment and suggests that uptake occurs on a homogeneous surface by monolayer sorption without interaction between adsorbed molecules. This model can be written as follows:[35]

$$q_e = \frac{q_{the} K_L C_e}{1 + K_L C_e} \quad (10)$$

where q_e is the adsorption capacity, mmol g^{-1}; C_e is the equilibrium concentration of metal ions, mmol L^{-1}; q_{the} is theoretical saturation adsorption capacity, mmol g^{-1}; and K_L is the Langmuir constant that is related to the affinity of binding sites, L $mmol^{-1}$. The linear expression of the Langmuir isotherm is eq 11:

$$\frac{C_e}{q_e} = \frac{C_e}{q_{the}} + \frac{1}{qK_L} \quad (11)$$

Nonlinear regression and graphical methods by plotting C_e/q_e vs C_e were used to evaluate the Langmuir parameters.

The Langmuir model parameters and fits of experimental data to the above equations are given in Table 4.

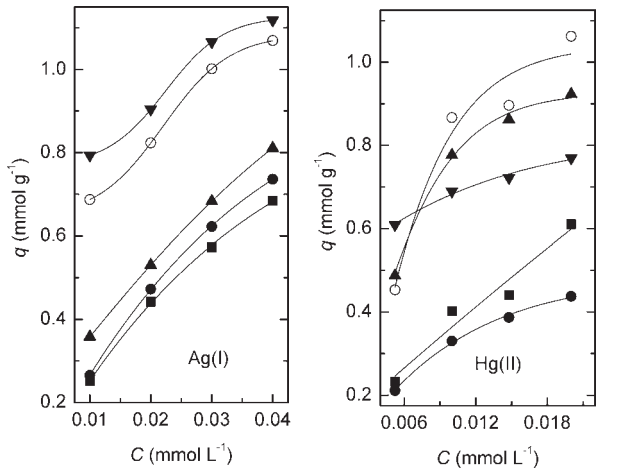

Figure 4. Isotherms for the adsorption of Ag(I) and Hg(II) ions onto adsorbents ■, SiO_2-EA; ●, SiO_2-DEA; ▲, SiO_2-EDA; ▼, SiO_2-DETA; and ○, SiO_2-TETA.

From Table 4, it can be seen that the regression coefficients R^2 of the linear and nonlinear Langmuir models are more than 0.93, suggesting that both the linear and nonlinear Langmuir isotherm models can be used to describe the adsorption of Ag(I) and Hg(II) ions onto the adsorbents SiO_2-EA, SiO_2-DEA, SiO_2-EDA, SiO_2-DETA, and SiO_2-TETA under the present conditions. According to R^2, some conclusions can also be drawn that from Table 4: (1) The nonlinear Langmuir model is suitable for describing the isotherm adsorption of Ag(I) onto SiO_2-EA, SiO_2-DEA, and SiO_2-EDA, and the linear Langmuir form is suitable for describing the isotherm adsorption of Ag(I) onto SiO_2-DETA and SiO_2-TETA. (2) The linear Langmuir model is more suitable than the nonlinear form for describing the isotherm adsorption of Hg(II) onto the five adsorbents.

The fact that the adsorption of the Ag(I) and Hg(II) onto SiO_2-EA, SiO_2-DEA, SiO_2-EDA, SiO_2-DETA, and SiO_2-TETA fitted well the Langmuir model indicated that the adsorption of the two metal ions on the five adsorbents takes place at the functional groups/binding sites on the surface of the adsorbents which can be regarded as monolayer adsorption.

The Freundlich isotherm, an empirical equation, is capable of describing the adsorption of organic and inorganic compounds on a wide variety of adsorbents. It proposes adsorption with a heterogeneous energetic distribution of active sites, accompanied by interactions between adsorbed molecules.[36] The Freundlich model is expressed as

$$q_e = K_F C_e^{1/n} \quad (12)$$

where K_F is the binding energy constant reflecting the affinity of the adsorbents to metal ions ($mmol^{1-(1/n)}$ $L^{1/n}$ g^{-1}) and n is the Freundlich exponent related to adsorption intensity. The linear expression of the Freundlich isotherm is eq 13:

$$\ln q_e = \ln K_F + \frac{\ln C_e}{n} \quad (13)$$

The constants, K_F and n, in the Freundlich isotherm are determined by linear regression, by plotting ln q_e vs ln C_e, as well as by nonlinear regression. Table 5 shows the linear and nonlinear Freundlich adsorption isotherm constants, K_F and n, and the

Table 4. Isotherm Parameters of the Langmuir Model for the Adsorption of Ag(I) and Hg(II) ions Obtained by Using the Linear Method and the Nonlinear Method

		Langmuir							
		linear regression				nonlinear regression			
adsorbents	metal ion	q_{the} (mmol g^{-1})	K_L (L $mmol^{-1}$)	R^2	χ^2	q_{the} (mmol g^{-1})	K_L (L $mmol^{-1}$)	R^2	χ^2
SiO_2-EA	Ag	1.54	20.70	0.9979	0.0000983	1.52	21.16	0.9996	0.0000963
SiO_2-DEA		1.73	19.37	0.9966	0.000159	1.69	20.13	0.9996	0.000150
SiO_2-EDA		1.38	35.57	0.9790	0.00234	1.42	33.35	0.9898	0.00228
SiO_2-DETA		1.29	161.00	0.9924	0.00720	1.25	186.80	0.9966	0.00593
SiO_2-TETA		1.31	110.51	0.9873	0.00707	1.27	122.42	0.9431	0.00624
SiO_2-EA	Hg	1.18	51.38	0.9350	0.00848	1.24	47.48	0.9429	0.00857
SiO_2-DEA		0.67	97.71	0.9965	0.000354	0.67	99.33	0.9964	0.000350
SiO_2-EDA		1.24	167.88	0.9882	0.00503	1.25	166.44	0.9706	0.00485
SiO_2-DETA		0.82	636.79	0.9983	0.00102	0.81	730.73	0.9629	0.000701
SiO_2-TETA		1.67	98.16	0.9473	0.0242	1.60	110.73	0.9467	0.0238

dx.doi.org/10.1021/je1009784 |J. Chem. Eng. Data 2011, 56, 1982–1990

Table 5. Isotherm Parameters of the Freundlich Model for the Adsorption of Ag(I) and Hg(II) Ions Obtained by Using the Linear Method and the Nonlinear Method

		Freundlich							
		linear regression				nonlinear regression			
		K_F				K_F			
adsorbents	metal ion	$(mmol^{1-(1/n)}\ L^{1/n}\ g^{-1})$	n	R^2	χ^2	$(mmol^{1-(1/n)}\ L^{1/n}\ g^{-1})$	n	R^2	χ^2
SiO_2-EA	Ag	7.22	1.31	0.9948	0.00139	6.39	1.46	0.9951	0.00139
SiO_2-DEA		8.26	1.36	0.9942	0.00182	7.18	1.44	0.9939	0.00183
SiO_2-EDA		5.29	1.73	0.9994	0.000119	5.42	1.71	0.9995	0.000120
SiO_2-DETA		2.43	4.21	0.9686	0.00218	2.48	4.13	0.9690	0.00218
SiO_2-TETA		2.95	3.23	0.9802	0.00207	3.01	3.18	0.9798	0.00206
SiO_2-EA	Hg	8.12	1.52	0.9622	0.00778	8.12	1.52	0.9518	0.00776
SiO_2-DEA		3.68	1.89	0.9792	0.00209	3.17	2.02	0.9791	0.00207
SiO_2-EDA		5.74	2.26	0.9677	0.0135	4.67	2.53	0.9706	0.0133
SiO_2-DETA		1.39	6.72	0.9931	0.00144	1.39	6.72	0.9925	0.00144
SiO_2-TETA		11.19	1.75	0.9980	0.0378	7.89	2.02	0.9966	0.0358

Table 6. Isotherm Parameters of the Redlich−Peterson Model for the Adsorption of Ag(I) and Hg(II) Ions

		Redlich−Peterson				
		A	B			
adsorbent	metal ion	$(L\ g^{-1})$	$(L\ mmol^{-(1-1/A)})$	g	R^2	χ^2
SiO_2-EA	Ag	32.15	21.16	1.0	0.9996	0.0000952
SiO_2-DEA		34.04	20.13	1.0	0.9996	0.000151
SiO_2-EDA		606.42	115.25	0.44	0.9995	0.000468
SiO_2-DETA		21766.98	8831.74	0.76	0.9688	0.00220
SiO_2-TETA		8479.98	2846.33	0.69	0.9796	0.00612
SiO_2-EA	Hg	934.53	117.93	0.36	0.9517	0.00876
SiO_2-DEA		66.51	99.33	1.0	0.9964	0.000365
SiO_2-EDA		208.72	166.44	1.0	0.9706	0.00484
SiO_2-DETA		5327.12	4030.05	0.86	0.9924	0.00158
SiO_2-TETA		177.11	110.73	1.0	0.9167	0.00238

regression coefficients, R^2. On the basis of the R^2 values, some conclusions can be drawn from Table 5: (1) Both linear and nonlinear Freundlich forms can be used to describe the isothermal adsorption of Ag(I) onto the five adsorbents because the R^2 values of the two forms are very close to or more than 0.97. In general, favorable adsorption tends to have a Freundlich constant n between 1 and 10. A larger value of n implies stronger interaction between the adsorbent and metal ion, while n equal to 10 indicates linear adsorption leading to identical adsorption energies for all sites.[37] It can be seen that the n values in Table 6 are between 1 and 10, suggesting that all of the adsorption processes for the two metal ions onto the five adsorbents were favorable. It also can be found from Table 6 that the n values of amino-terminated adsorbents toward Ag(I) and Hg(II) were always higher than those of hydroxyl-terminated ones (except SiO_2-TETA toward Hg(II)), indicating that the amino groups exhibited stronger interactions than hydroxyl groups with the two kinds of metal ions.

The Redlich−Peterson equation is another empirical expression involving three parameters, A $(L\ g^{-1})$, B $(L\ mmol^{1-(1/A)})$, and g $(0 < g < 1)$, which is capable of representing adsorption equilibrium over a wide concentration range.[38] A and B are the Redlich−Peterson isotherm constants, and g is the degree of heterogeneity. When the coverage is very low, eq 14 becomes linear and leads to Henry's Law. For high coverage, eq 14 can be assimilated to the Freundlich equation,[39] since the ratio A/B and $(1 - g)$ corresponds to the parameters K_F and $1/n$ of the Freundlich isotherm (eq 13). For $g = 1$, it can be assimilated to the Langmuir equation,[40] where A/B is numerically equal to the monolayer capacity (Q_0) and B is the adsorption equilibrium constant.

$$q_e = \frac{AC_e}{1 + BC_e^g} \tag{14}$$

The experimental data were fitted to the Redlich−Peterson equation by applying nonlinear regression analysis. The calculated isotherm constants are given in Table 7, and showed that the Redlich−Peterson model gave higher regression coefficients (>0.95). From Tables 4, 5, and 6, it can be observed that the R^2 value for the Redlich−Peterson isotherm was found to be more

Table 7. The Desorption of Ag(I) and Hg(II) from Adsorbents SiO_2-EA, SiO_2-DEA, SiO_2-EDA, SiO_2-DETA, and SiO_2-TETA

	Ag	Hg
adsorbents	(%)	(%)
SiO_2-EA	96.34	99.98
SiO_2-DEA	93.61	100
SiO_2-EDA	93.11	100
SiO_2-DETA	94.35	100
SiO_2-TETA	99.90	98.06

or less nearer to the best-fit Langmuir and Freundlich isotherm equations. In addition, Tables 4 and 6 show that the regression coefficients of the Redlich−Peterson and Langmuir isotherms have the same values in some cases and seemed to be the best-fitting models for the experimental results. Thus, the Langmuir isotherm is a special case of the Redlich−Peterson isotherm when the constant g is unity.

Comparing the R^2 values of the three above-mentioned isotherm models, it is easy to find that the Langmuir, Freundlich, and Redlich−Peterson isotherms can be used to describe the experimental data of Ag(I) and Hg(II) adsorption onto SiO_2-EA, SiO_2-DEA, SiO_2-EDA, SiO_2-DETA, and SiO_2-TETA. This fact shows that the five adsorbents have similar adsorption mechanisms to the two metal ions, and all of them are attributed to monolayer adsorption and chemisorption.[41]

In this study, the chi-square test was also used to evaluate the fit of the isotherms to the experimental equilibrium data. The chi-square test statistic is basically the sum of the squares of the differences between the experimental data and data obtained in a calculation using the models, with each squared difference divided by the corresponding data obtained by calculating from models. The equivalent mathematical statement is[42]

$$\chi^2 = \sum \frac{(q_{exp} - q_{the})^2}{q_{the}} \quad (15)$$

where q_{the} is the equilibrium capacity obtained by calculating from the model (mmol/g) and q_{exp} is experimental data of the equilibrium capacity (mmol/g). If data from the model are similar to the experimental data, χ^2 will be a small number; if they are different, χ^2 will be a large number.

The chi-square statistic, χ^2, was obtained and is shown in Tables 4, 5, and 6. All of the values of χ^2 are relatively small (<0.1). In the chi-square analysis of Ag(I), the χ^2 of the nonlinear Langmuir isotherms exhibited lower values than those of the linear Langmuir model. The Redlich−Peterson isotherms exhibited lower χ^2 values than the Langmuir and the Frendlich isotherms, which was considered to be a better fit compared to Langmuir and the Frendlich. But regarding Hg(II), χ^2 of the Frendlich isotherms whose constants were obtained from the linear forms and the nonlinear forms were almost identical. Meanwhile, Frendlich isotherms have higher χ^2 values than the Langmuir and the Redlich−Peterson isotherms. Therefore, drawing conclusions from the chi-square statistic, the Redlich−Peterson isotherm was the best-fitting isotherm for Ag(I) and the Frendlich isotherm for Hg(II).

3.4. Primary Desorption. According to our previous work,[43] 5 % thiourea in 0.5 mol L^{-1} HNO_3 was chosen as the eluent to be used in the primary desorption experiment of the adsorbents, and the results are shown in Table 7. It can be seen that Ag(I) and Hg(II) loaded on the adsorbents could be easily eluted. Details related to the regeneration and dynamic adsorption of the adsorbents will be further investigated in a future article.

4. CONCLUSIONS

The present study focused on the adsorption of Ag(I) and Hg(II) onto silica gel with functional groups of hydroxyl- or amino-terminated polyamine adsorbents SiO_2-EA, SiO_2-DEA, SiO_2-EDA, SiO_2-DETA, and SiO_2-TETA, and the following conclusions were drawn:

(1) The adsorption kinetic processes study indicated that a pseudo-second-order rate model provided an excellent fitting for Ag(I) and Hg(II) adsorption onto adsorbents SiO_2-EA, SiO_2-DEA, SiO_2-EDA, SiO_2-DETA, and SiO_2-TETA. Film diffusion might be dominant in the adsorption process of Ag(I) and Hg(II) onto the five adsorbents. The species of terminal groups and cross-linking structure of the functional groups have a significant effect on the adsorption rate and initial rate of metal ions onto the adsorbents.

(2) The linear and nonlinear Langmuir, Freundlich, and Redlich−Peterson isotherm models can be used to fit the experimental data and to predict the adsorption equilibrium for Ag(I) and Hg(II) onto SiO_2-EA, SiO_2-DEA, SiO_2-EDA, SiO_2-DETA, and SiO_2-TETA. The Redlich−Peterson isotherm was the best-fitting isotherm for Ag(I) and the Frendlich isotherm for Hg(II). The Redlich−Peterson model is a special case of the Langmuir isotherm when the Redlich−Peterson isotherm constant g is unity.

(3) Ag(I) and Hg(II) loaded on the adsorbents SiO_2-EA, SiO_2-DEA, SiO_2-EDA, SiO_2-DETA, and SiO_2-TETA can be easily regenerated by a 5 % thiourea 0.1 mol L^{-1} HNO_3 solution.

AUTHOR INFORMATION

Corresponding Author

*Corresponding author. Tel.: +86 535 6699201. E-mail: rongjunqu@sohu.com or qurongjun@eyou.com.

Funding Sources

The authors are grateful for the financial support by the National Natural Science Foundation of China (Grant No.51073075), Natural Science Foundation of Shandong Province (No. 2009ZRB01463, 2008BS04011, Y2007B19), the Nature Science Foundation of Ludong University (No.08-CXA001, 032912, 042920, LY20072902), and the Educational Project for Postgraduate of Ludong University (No. YD05001, Ycx0612).

REFERENCES

(1) Akgül, M.; Karabakan, A.; Acar, O.; Yürüm, Y. Removal of silver (I) from aqueous solutions with clinoptilolite. *Microporous Mesoporous Mater.* **2006**, *94*, 99–104.

(2) Cotton, F. A.; Wilkinson, G. *Advanced Inorganic Chemistry*; Interscience Publishers: New York, 1980.

(3) Hasan, S.; Ghosh, T. K.; Viswanath, D. S.; Boddu, V. M. Dispersion of chitosan on perlite for enhancement of copper(II) adsorption capacity. *J. Hazard. Mater.* **2008**, *152*, 826–837.

(4) Igwe, J. C.; Abia, A. A.; Ibeh, C. A. Adsorption kinetics and intraparticulate diffusivities of Hg, As and Pb ions on unmodified and thiolated coconut fiber. *Int. J. Environ. Sci. Technol.* **2008**, *5*, 83–92.

(5) Guibal, E. Interactions of metal ions with chitosan-based sorbents: a review. *Sep. Purif. Technol.* **2004**, *38*, 43–74.

(6) Ruparelia, J. P.; Duttagupta, S. P.; Chatterjee, A. K.; Mukherji, S. Potential of carbon nanomaterials for removal of heavy metals from water. *Desalination* **2008**, *232*, 145–156.

(7) Deligöz, H.; Erdem, E. Comparative studies on the solvent extraction of transition metal cations by calixarene, phenol and ester derivatives. *J. Hazard. Mater.* **2008**, *154*, 29–32.

(8) Vijayalakshmi, A.; Arockiasamy, D. L.; Nagendran, A.; Mohan, D. Separation of proteins and toxic heavy metal ions from aqueous solution by CA/PC blend ultrafiltration membranes. *Sep. Purif. Technol.* **2008**, *62*, 32–38.

(9) Atia, A. A.; Donia, A. M.; Elwakeel, K. Z. Selective separation of mercury (II) using a synthetic resin containing amine and mercaptan as chelating groups. *React. Funct. Polym.* **2005**, *65*, 267–275.

(10) Türker, A. R. New sorbents for solid-phase extraction for metal enrichment. *Clean* **2007**, *35*, 548–557.

(11) Jal, P. K.; Patel, S.; Mishra, B. K. Chemical modification of silica surface by immobilization of functional groups for extractive concentration of metal ions. *Talanta* **2004**, *62*, 1005–1028.

(12) Hassanien, M. M.; Abou-El-Sherbini, K. S. Synthesis and characterisation of morin-functionalised silica gel for the enrichment of some precious metal ions. *Talanta* **2006**, *68*, 1550–1559.

(13) Lam, K.F.; Yeung, K. L.; Mckay, G. Efficient approach for Cd^{2+} and Ni^{2+} removal and recovery using mesoporous adsorbent with tunable selectivity. *Environ. Sci. Technol.* **2007**, *41*, 3329–3334.

(14) Gübbük, H.; Güp, R.; Ersöz, M. Synthesis, characterization, and sorption properties of silica gel-immobilized Schiff base derivative. *J. Colloid Interface Sci.* **2008**, *320*, 376–382.

(15) Gao, B. J.; An, F. Q.; Liu, K. K. Studies on chelating adsorption properties of novel composite material polyethyleneimine/silica gel for heavy-metal ions. *Appl. Surf. Sci.* **2006**, *253*, 1946–1952.

(16) Sales, J. A. A.; Prado, A. G. S.; Airoldi, C. The incorporation of propane-1,3-diamine into silylant epoxide group through homogeneous and heterogeneous routes. *Polyhedron* **2002**, *21*, 2647–2651.

(17) Sales, J. A. A.; Airoldi, C. Calorimetric investigation of metal ion adsorption on 3-glycidoxypropyltrimethylsiloxane + propane-1, 3-diamine immobilized on silica gel. *Thermochim. Acta* **2005**, *427*, 77–83.

(18) Yoshitake, H.; Koiso, E.; Horie, H.; Yoshimura, H. Polyamine-functionalized mesoporous silicas: Preparation, structural analysis and oxyanion adsorption. *Microporous Mesoporous Mater.* **2005**, *85*, 183–194.

(19) Liu, C. K.; Bai, R. B.; Hong, L. Diethylenetriamine-grafted poly(glycidyl methacrylate) adsorbent for effective copper ion adsorption. *J. Colloid Interface Sci.* **2006**, *303*, 99–108.

(20) Liu, C. K.; Bai, R. B.; Ly, Q. S. Selective removal of copper and lead ions by diethylenetriamine-functionalized adsorbent: Behaviors and mechanisms. *Water Res.* **2008**, *42*, 1511–1522.

(21) Atia, A. A.; Donia, A. M.; Awed, H. A. Synthesis of magnetic chelating resins functionalized with tetraethylenepentamine for adsorption of molybdate anions from aqueous solutions. *J. Hazard. Mater.* **2008**, *155*, 100–108.

(22) Zhang, Y.; Qu, R. J.; Sun, C. M.; Qu, B. H.; Sun, X. Y.; Ji, C. N. End-group protection as a novel strategy to prepare silica-gel supported diethylenetriamine with high adsorption capacities for metal ions. *J. Non-Cryst. Solids* **2009**, *355*, 453–457.

(23) Zhang, Y.; Qu, R. J.; Sun, C. M.; Wang, C. H.; Ji, C. N.; Chen, H.; Yin, P. Chemical modification of silica-gel with diethylenetriamine via an end-group protection approach for adsorption to Hg(II). *Appl. Surf. Sci.* **2009**, *255*, 5818–5826.

(24) Qu, R. J.; Wang, M. H.; Sun, C. M.; Zhang, Y.; Ji, C. N.; Chen, H.; Meng, Y. F.; Yin, P. Chemical modification of silica-gel with hydroxyl- or amino-terminated polyamine for adsorption of Au(III). *Appl. Surf. Sci.* **2008**, *255*, 3361–3370.

(25) Boyd, G. E.; Adamson, A. W.; Myers, L. S. The exchange adsorption of ions from aqueous solutions by organic zeolites. II. Kinetics. *J. Am. Chem. Soc.* **1947**, *69*, 2836–2848.

(26) Reichenberg, D. Properties of ion-exchange resins in relation to their structure III, kinetics of exchange. *J. Am. Chem. Soc.* **1953**, *75*, 589–592.

(27) Helfferich, F. *Ion-Exchange*; McGraw Hill: New York, 1962.

(28) Mohan, D.; Singh, K. P. Single- and multi-component adsorption of cadmium and zinc using activated carbon derived from bagasse—an agricultural waste. *Water Res.* **2006**, *36*, 2304–2318.

(29) El-Kamash, A. M.; Zaki, A. A.; Abed-El-Geleel, M. Modeling batch kinetics and thermodynamics of zinc and cadmium removal from waste solutions using synthetic zeolite. *J. Hazard. Mater.* **2005**, *127*, 211–220.

(30) Barkat, M.; Nibou, D.; Chegrouche, S.; Mellah, A. Kinetics and thermodynamics studies of chromium(VI) ions adsorption onto activated carbon from aqueous solutions. *Chem. Eng. Process* **2009**, *48*, 38–47.

(31) Ho, Y. S.; McKay, G.; Wase, D. A. J.; Foster, C. F. Study of the sorption of divalent metal ions on to peat. *Adsorp. Sci. Technol.* **2000**, *18*, 639–650.

(32) Brusseau, M. L.; Rao, P. S. C. Sorption non-ideality during organic contaminant transport in porous media. *CRC Crit. Rev. Environ. Control* **1984**, *19*, 33–99.

(33) Ho, Y. S. Second-order kinetic model for the sorption of cadmium onto tree fern: a comparison of linear and non-linear methods. *Water Res.* **2006**, *40*, 119–125.

(34) Kumar, K. V.; Sivanesn, S. Comparative analysis of linear and non-linear method of estimating the sorption isotherm parameters for malachite green onto activated carbon. *J. Hazard. Mater. B* **2006**, *136*, 197–202.

(35) Sari, A.; Mendil, D.; Tuzen, M.; Soylak, M. Biosorption of palladium(II) from aqueous solution by moss (Racomitrium lanuginosum) biomass: Equilibrium, kinetic and thermodynamic studies. *J. Hazard. Mater.* **2009**, *162*, 874–879.

(36) Ramesh, A.; Hasegawa, H.; Sugimoto, W.; Maki, T.; Ueda, K. Adsorption of gold(III), platinum(IV) and palladium(II) onto glycine modified crosslinked chitosan resin. *Bioresour. Technol.* **2008**, *99*, 3801–3809.

(37) Febrianto, J.; Kosasiha, A. N.; Sunarso, J.; Ju, Y. H.; Indraswati, N.; Ismadji, S. Equilibrium and kinetic studies in adsorption of heavy metals using biosorbent: A summary of recent studies. *J. Hazard. Mater.* **2009**, *162*, 616–645.

(38) Redlich, O.; Peterson, D. L. A useful adsorption isotherm. *J. Phys. Chem.* **1959**, *63*, 1024–1024.

(39) Zhou, M. L.; Martin, G.; Taha, S.; Sant'anna, F. Adsorption isotherm comparison and modelling in liquid phase onto activated carbon. *Water Res.* **1996**, *32*, 1109–1118.

(40) Ho, Y. S.; Huang, C. T.; Huang, H. W. Equilibrium sorption isotherm for metal ions on tree fern. *Proc. Biochem.* **2002**, *37*, 1421–1430.

(41) Sun, C. M.; Qu, R. J.; Ji, C. N.; Wang, C. H.; Sun, Y. Z.; Yue, Z. W.; Cheng, G. X. Preparation and adsorption properties of cross-linked polystyrene-supported low-generation diethanolamine-typed dendrimer for metal ions. *Talanta* **2006**, *70*, 14–19.

(42) Ho, Y S; Chiu, W T; Wang, C C. Regression analysis for the sorption isotherms of basic dyes on sugarcane dust. *Bioresour. Technol.* **2005**, *96*, 1285–1291.

(43) Qu, R. J.; Liu, J. H.; Sun, C. M.; Zhang, Y.; Ji, C. N.; Yin, P. Removal and separation of Hg(II) ions from aqueous solutions by macroporous polystyrene-co-divinylbenzene-supported polyamine chelating resins. *J. Chem. Eng. Data* [Online] DOI: 10.1021/je100246y.